Nano World Journal

https://doi.org/10.17756/nwj.2023-s2-018

Research Article

Open Access

Strength of Unfired Clay Bricks with Almond Husk Additive in Relation to Surface Porosity Based on a Quantification by SEM Images Analysis

Othmane Noureddine[1], Imad Manssouri[1], Hassane Sahbi[2], Houssame Limami[3] and Asmae Khaldoun[3]

[1]*Laboratory of Mechanics, Mechatronics, and Command, Team of Electrical Energy, Maintenance and Innovation, ENSAM-Meknes, Moulay Ismail University, Marjane 2, BP:15290 Meknes, Morocco*

[2]*Moulay Ismail University, Marjane 2, BP: 298, Presidency Meknes, Morocco*

[3]*Laboratory of Sustainable Energy Materials, Al Akhawayn University, Ifrane, Morocco*

***Correspondence to:**
Othmane Noureddine
Laboratory of Mechanics, Mechatronics, and Command,
Team of Electrical Energy, Maintenance and Innovation,
ENSAM-Meknes, Moulay Ismail University,
Marjane 2, BP:15290 Meknes, Morocco.
E-mail: oth.noureddine@gmail.com

Received: July 25, 2023
Accepted: September 22, 2023
Published: September 25, 2023

Citation: Noureddine O, Manssouri I, Sahbi H, Limami H, Khaldoun A. 2023. Strength of Unfired Clay Bricks with Almond Husk Additive in Relation to Surface Porosity Based on a Quantification by SEM Images Analysis. *NanoWorld J* 9(S2): S102-S106.

Copyright: © 2023 Noureddine et al. This is an Open Access article distributed under the terms of the Creative Commons Attribution 4.0 International License (CCBY) (http://creativecommons.org/licenses/by/4.0/) which permits commercial use, including reproduction, adaptation, and distribution of the article provided the original author and source are credited.

Published by United Scientific Group

Abstract

Aiming to reduce the resources invested in the laboratory assessment of unfired clay bricks incorporating natural wastes as additives, this paper proposes an evaluation of the surface porosity of unfired clay bricks with almond husk powder using processing of the SEM (Scanning electron microscope) images of representative cubes and its relationship with the bricks' strength. Used clay is extracted from Bensmim red soil in Ifrane - Morocco and determined as an Illite. One control specimen with pure clay and four specimens were prepared using the proportions 2, 5, 10, and 20 wt.% of almond husk powder. After drying, SEM analysis is done on the specimens. The processing of the issued images is done using ImageJ software. The results show, in general, an increase in the surface porosity with the increase of almond husk powder in the matrix. This is reported due to the formation of coagulant volumes that generates a porous network depending on the size and the amount of the additive. However, a considerable decrease in the porosity is shown using 2 wt.% additive which is reported to the fiber bridging mechanism. The increase in the surface porosity was followed by an increase in strength. Theoretical models are evaluated for the best fit in the relationship between strength and porosity. Nevertheless, the polynomial modeling of degree 3 is considered the most adequate. The findings in this research establish a potential road to predict unfired clay bricks quality using the processing of SEM images of only representative specimens of the surface porosity.

Keywords

Unfired clay bricks, Compressive strength, Surface porosity, SEM images processing

Introduction

Hundreds of works are investigating the physicochemical, thermal, and mechanical properties of unfired bricks made from earth and waste materials as additives. In a global context of the increase in the cost of production of construction materials energy and increase of its carbon dioxide emissions [1], this old alternative is considered an interesting approach to follow, especially with the coming expected housing need. 96,000 new affordable homes need to be built every day to cover the need by 2030 [2]. Governmental and non-governmental organizations are putting together strategies based on last scientific findings to overcome these challenges. However, this global dynamism must be accompanied by innovative laboratory experimental techniques. In fact, testing undried clay bricks incorporated requires massive resources: depending on the adopted international standard, it is demanded to evaluate several samples for each spec-

imen to have representative results; unfiring the bricks means time-consuming and storing them in adequate conditioning environments. This implies money, effort, and time spending.

The literature shows three approaches aiming to suggest prediction methods for various technological properties of construction materials: first, using methods of artificial intelligence. Compressive strength prediction models of alkali-activated construction demolition waste geopolymers were constructed based on three machine learning algorithms; the results applicability was confirmed with high precision [3]. Limami et al. analyzed the modeling of a forecasting technique, through machine learning and linear regression, intending to predict bricks' thermal, mechanical, and physicochemical properties at different HDPE and PET plastic waste additive percentages. A good correlation was found between the suggested models and the experimental findings [4]. Secondly, experimental approaches that are based on rheological measurements. In a previous study, a linear correlation was found between the compressive strength of unfired clay bricks with almond husk powder and the storage modulus in the linear viscoelastic range of suspensions made from the same raw materials. The correlation showed strong coefficients of determination ($R^2 > 0.92$). This demonstrates the possibility of assessing and estimating unfired bricks' strength behavior using only rheometry measurements [5]. The third kind of attempt to predict the behavior of bricks' strength is the investigation of the inter-relationships to the physicochemical properties; in particular, the porosity. In various studies [6], the porosity level in bricks is found a crucial parameter to define the compressive strength of bricks. For instance, in Limami et al.'s study about the reinforcement of unfired bricks using 20 wt.% typha fiber as an additive in bricks, apparent porosity goes to 14.95%, compared with control brick (1.14%) [7]. Pores are voids created in the matrix due to the creation of interlayer spacings between constituted flocculants and/or clay particles and/or any additive materials [7, 8]. Thus, the particles size and proportion of each material define a porosity level, therefore bricks' strength. Theoretical mathematical models that were formerly developed have been reported in the literature.

The most famous relationship is Balshin model which is applicable in ceramics with very high silicon dioxide quartz content. Balshin model is expressed with the relation [9]:

$$\sigma = \sigma_0 \left(1 - p\right)^b$$

Where, σ is the compressive strength, σ_0 is the compressive strength of the brick at a non-porous (zero porosity) state; σ_0 is obtained using a statistical regression of experimental strength measurements, and p is the measured porosity points. Finally, b represents an empirical constant.

In the case of low porosity materials rich in Al_2O_3, Ryshkewitch suggests the equation [9]:

$$\sigma = \sigma_0 e^{-kp}$$

Where, b represents an empirical constant.

In the case of materials rich of calcium, Schiller is considered the best fitting model with the logarithmic equation [9]:

$$\sigma = n.\ln\left(p_0/p\right)$$

Where, p_0 is the porosity of the brick at zero strength; p_0 is obtained using a statistical regression of experimental porosity measurements. n represents an empirical constant.

The simplest model is Hasslman's, which linearly links the bricks' strength to the porosity by the equation [9]:

$$\sigma = \sigma_0 - c.p$$

Where, c represents an empirical constant.

The most reliable method to evaluate the apparent porosity is using the gravimetric Archimedes model that is described in the ASTM C20-00 standard. The latter consists of submerging the test specimens in boiling water for a two-hour period and measuring the corresponding weights to make the calculations according to the standard. However, this method is not suitable for unfired bricks because their matrix is more water-absorbent which leads to the complete destruction of the brick. This is one of the weakest properties in unfired clay bricks that restrict their usage. SEM Images analysis for porosity calculation is a recent approach to overcome the inconveniences of water testing. Chinchillas-Chinchillas et al. used the NI Vision Assistant software to analyze the percentage of porosity and representative results were achieved [10]. Zeil et al. evaluated SEM images with a Leica Quantimet 500 image analysis system and were able to calculate the 'porous area fraction' defined as the ratio of the area of the pores to the total area of the analyzed image [11].

This paper synthesizes the just introduced approaches and findings through a study of the feasibility of using SEM images processing as a means to predict the compressive strength of unfired clay bricks with almond husk powder as an additive. The novelty in this work is the evaluation of different theoretical models of the porosity-compressive strength relationship using the surface porosity issued from SEM images of the studied bricks.

Materials and Method

Materials

The clay is extracted from Bensmim red soil in Ifrane – Morocco. Previously used in several research, this clay showed its suitability for earthen construction materials [12-14]. In conformity with ASTM D5357, X-ray diffraction is performed on the studied clay. The mineralogical composition is shown in figure 1. Quartz of silicon dioxide predominates. The used clay is considered non-swelling with low plasticity nature due to the presence of Illite/Muscovite [15, 16]. The X-ray fluorescence analysis performed on Bensmim soil, in previous studies, proved the presence of aluminum oxide (Al_2O_3) confirming the clayey portion [17]. Calcite and Dolomite are present with low content. Used materials are nanomaterials.

Almond husk was collected and used as an additive in the manufacturing of specimens. According to the literature [18], the husk is constituted of various elements that made

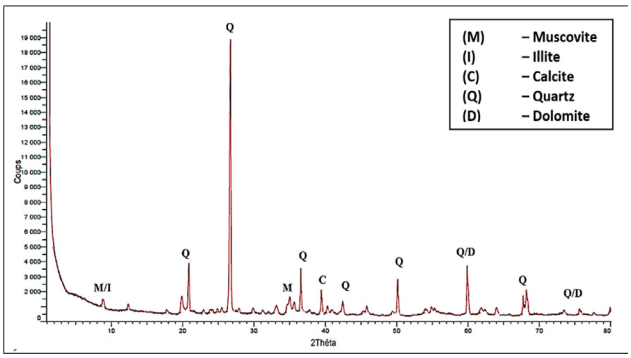


Figure 1: X-ray Diffraction of extracted soil: (M) - Muscovite, (I) - Illite, (C) - Ialcite, (Q) - Quartz, and (D) - Dolomite.

it suitable as feed for animals. The composition is as follows: Cellulose (20.6 - 35.2 wt.%), hemicellulose (about 10 wt.%), lignin (7.5 - 15.6 wt.%), an important portion of soluble sugars (18.0 - 30.0 wt.%) and protein content (2.1 - 8.8 wt.%). The used almond husk was tested for its density at 0% moisture contents according to ASTM D2395 - Test Method B and found to be 0.725 g/cm^3.

Method

Raw materials were prepared to form cube specimens of 10 mm in the edge. The soil was cleansed, dried to eliminate moisture, crushed, and then sieved at 100 µm. Equally, the almond husk is ground and sieved at 100 µm. 2, 5, 10, and 20 wt.% almond husk is incorporated into clay, then mixed for 5 minutes using an electric mixer that animates Blade rotative movements (140 rpm) and planetary rotative movements (62 rpm). 16.5% water content was added to the mixture. This optimum moisture content is found using the proctor compaction test following the ASTM D698 standard, at 5 MPa applied pressure. The mixing continued for an additional 5 minutes. The specimens were finally molded and went into the drying process. The latter consists of three-phase drying. The first is in a 25 °C ± 1 °C control room for 18 days. The second is in an oven at a temperature starting from 30 °C to 60 °C with a 5 °C/h increment factor; making it 6 hours, then cooled in a 25 °C ± 1 °C control room for 3 days. This intermediate drying aims to mitigate moisture content that weakened the resistance specimens [19]. The final drying is in an oven, for 24 hours, at a temperature starting from 50 °C to 105 °C with a 10 °C/h increment factor, then cooled in a 25 °C ±1 °C control room. A control specimen was prepared as a reference.

For the specimens' surface observation and analysis, a high-vacuum mode is applied in JSM-IT500HR SEM. The SEM images processing is done using ImageJ open-source software. The analysis consists of first adapting the images. The threshold intensity is defined for each image. The software calculates then the fraction of area showing pores, thus the surface porosity.

Corresponding bricks were prepared according to the same procedure, tested for their compressive strength conforming to ASTM C1314 and presented in an earlier study [5]. Figure 2 shares the results where it was found a slight enhancement in the bricks' strength when incorporating 2 wt.% of almond husk powder. The reached gain at this optimum content was

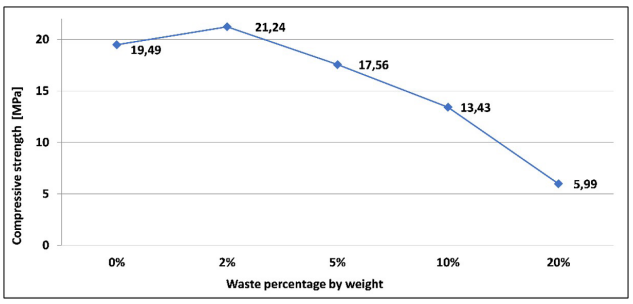


Figure 2: Compressive strength of unfired bricks with almond husk powder for different weight percentages.

estimated to be 8.98% compared to the control specimen. It was reported that this increase is due to the phenomenon of the fiber bridging mechanism which is responsible for increasing the friction between fibers and clay [20]. The compressive strength of the bricks dropped after the incorporation of additional amounts of almond husk content.

Results and Discussion

The performed SEM images on representative cubes of unfired clay bricks with 0, 2, 5, 10, and 20 wt.% almond husk powder as an additive are shown in figure 3. Different information could be determined using the images. The microstructure is constituted of irregular plate clay particles. The platelets are oriented parallelly in a way to form aggregates that are domains with irregular sizes due to the interaction effects of clay-hull and clay-shell [21]. Despite they are not shown in the image, almond husk granular particles are

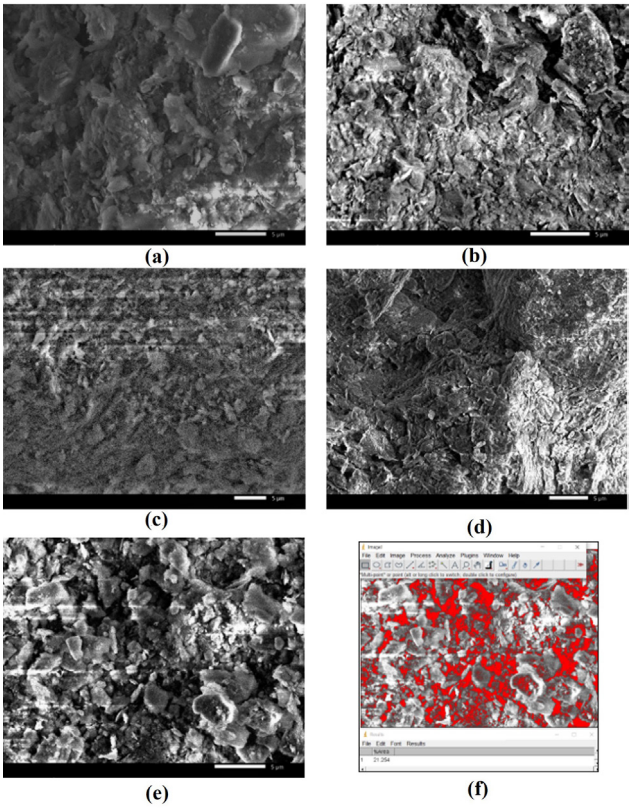


Figure 3: SEM images of prepared specimens with **(a)** 0, **(b)** 2, **(c)** 5, **(d)** 10, and **(e)** 20 wt.% additive and **(f)** image (e) processing using ImageJ.

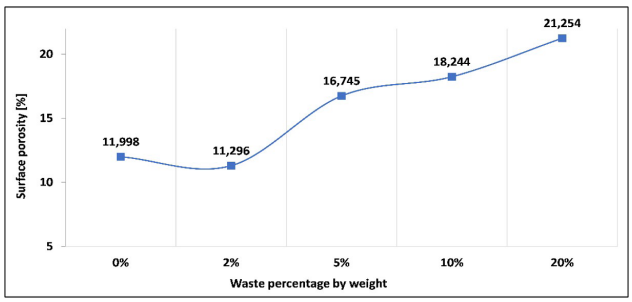


Figure 4: Surface porosity of representative cubes of unfired bricks with almond husk powder for different weight percentages.

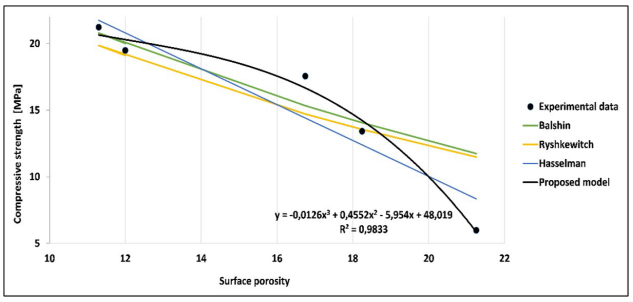


Figure 5: The compressive strength-porosity dependence. Representation of the Balshin, Ryshkewitch, and Hasslman models.

responsible for creating these flocculating volumes. This was observed during the preparation of the specimens. Each almond husk proportion incorporated into the mixture, there were produced coagulant particles of distinct volumes. Consequently, a distinct porous network is generated for each almond husk proportion. In fact, the higher the proportion of additives, the higher the number of coagulants, producing more pores [17].

To confirm this, micro-superficial porosity is evaluated using ImageJ processing images software (Figure 3f). The surface porosity as a function of the almond husk content is presented in figure 4. The pores are at their highest level (21.254%) in the specimens incorporating 20 wt.% additive, which complies with the latter explanation. However, the lower surface porosity level is recorded at 2 wt.% almond husk (11.296%), then it increases with the incorporation of the additive. The obtained minimum porosity is due to a phenomenon called the fiber bridging mechanism. It occurs in the of case randomly oriented soft fiber in a clay matrix [20] and it binds soil grains together more rigidly leading to less porosity creation up to an optimum content of the additive (2 wt.% in this study) [22].

The porosity evaluation by SEM (Figure 3) is found in accordance with the results from the bricks' strength testing (Figure 2). Table 1 shows a summary of the results. Pores creation is the main reason for the strength decrease in materials. At the minimum obtained surface porosity, the bricks are at their optimum strength. Similar conclusions are found in the literature. Limami et al. observed the relationship between porosity and compressive strength of unfired clay bricks incorporating typha fibers [7]. The reviews of Jannat et al. [6, 23] and Al-Fakih et al. [24] reported the same behavior of bricks' strength with respect to the pore's creation.

Table 1: Summary table of the results according to the composition of the bricks.

Waste percentage by weight	Surface porosity [%]	Compressive strength [MPa]
0%	11.998	19.49
2%	11.296	21.24
5%	16.745	17.56
10%	18.244	13.43
20%	21.254	5.99

The collected findings from the surface porosity evaluation by SEM images processing are used to correlate between these experimental findings and theoretically predicted results of compressive strength. Balshin, Ryshkewitch, and Hasslman are the three best-fitting models found in the literature and are initiated in the introduction of this article. Figure 5 presents the experimental findings on compressive strength-porosity dependence with the representation of the three models. The compressive strength of the brick at a non-porous (zero porosity) state σ_0 is obtained using a statistical linear regression of the experimental strength measurements. Hasslman model shows the most accurate prediction since it shows a correlation of R^2 = 0.943 compared to Balshin and Ryshkewitch (R^2 = 0.902 and R^2 = 0.887, respectively). The constants in each of these models represent a specific meaning and contribute primally to the construction of the equation. For instance, in the model of Balshin, fixing the empirical value of b is a way to have the best fit and it is related to the stress concentration factor around pores in the materials. It depends on the pore geometry and orientation in relation to the direction of application of the stress [9]. The Hasselman model assumes that the continuous phase of materials contains a dispersed phase of spherical particles, which is exactly our case where the dispersed phase consists of pores. The porosity in unfired bricks is considered high compared to the other porous materials. Therefore, pores acquire elastic properties to be equal to zero [25]. This makes the Hasselman model able to describe the most compressive strength in relation to porosity. For our particular case, it a behavior of inflection point curve was observed on the plotted data. This made us think to use a cubic polynomial regression with the equation mentioned in figure 5. The equation shows a very strong correlation of R^2 = 0.983. The detected inflection point behavior of the results of this study may be reported to a specific capacity of the brick, when exceeding it a catastrophic failure is triggered.

Conclusion

A new approach is introduced in this article of the evaluation of the compressive strength of unfired clay bricks with waste materials as additive. Specimens are prepared and analyzed in terms of microstructure using SEM images. The latter are processed using ImageJ software to quantify the surface porosity which is a key factor to define the bricks strength. The results showed less pores creation when incorporating 2 wt.% additive into the clay which was due to interarticular phenomena. The pores forming reduced the compressive

strength of the bricks. Using three of the most know models - Balshin, Ryshkewitch, and Hasslman models, correlations are established to the experimental findings. Very satisfying model fittings are obtained. However, a cubic polynomial regression is considered the most adapted to this case. The present study will contribute highly to the construction of a suitable prediction model for the strength of unfired clay bricks incorporating various natural additives. This is achievable through SEM images of only representative specimens and polynomial regression. As per recommendation, more studies need to focus on further verification of the direct match of this application and on defining the constants parameters of the regressions able to predict the unfired clay bricks' behavior.

Acknowledgments

None.

Conflict of Interest

None.

References

1. 2020 Global Status Report for Buildings and Construction: Towards a Zero-emissions, Efficient and Resilient Buildings and Construction Sector - Executive Summary. [https://wedocs.unep.org/handle/20.500.11822/34572;jsessionid=FED7512DDD04E3F32323D-4D65EF98748] [Accessed September 25, 2023]
2. Annual Report 2021. UN Habitat. [https://unhabitat.org/annual-report-2021] [Accessed September 25, 2023]
3. Shen J, Li Y, Lin H, Li H, Lv J, et al. 2022. Prediction of compressive strength of alkali-activated construction demolition waste geopolymers using ensemble machine learning. *Constr Build Mater* 360: 129600. https://doi.org/10.1016/j.conbuildmat.2022.129600
4. Limami H, Guettioui D, Dahi O, Manssouri I, El Alami A, et al. 2023. Machine learning forecasting of thermal, mechanical and physicochemical properties of unfired clay bricks with plastic waste additives. *Mater Today Proc* 72: 3509-3513. https://doi.org/10.1016/j.matpr.2022.08.218
5. Noureddine O, Manssouri I, Cherkaoui K, Sahbi H, Limami H, et al. 2022. Viscoelastic measurements of clay suspensions and their relationship to strength of unfired clay bricks with almond husk additive. *Int J Eng Res Africa* 61: 231-244. https://doi.org/10.4028/p-1p1oy2
6. Jannat N, Hussien A, Abdullah B, Cotgrave A. 2020. Application of agro and non-agro waste materials for unfired earth blocks construction: a review. *Constr Build Mater* 254: 119346. https://doi.org/10.1016/j.conbuildmat.2020.119346
7. Limami H, Manssouri I, Cherkaoui K, Khaldoun A. 2021. Mechanical and physicochemical performances of reinforced unfired clay bricks with recycled Typha-fibers waste as a construction material additive. *Clean Eng Technol* 2: 100037. https://doi.org/10.1016/j.clet.2020.100037
8. El-Yahyaoui A, Manssouri I, Noureddine O, Sahbi H, Khaldoun A. 2023. Physical and mechanical properties of unfired clay bricks with saw palmetto fibers additive as a construction material. *Mater Today Proc* 72: 3804-3814. https://doi.org/10.1016/j.matpr.2022.09.487
9. Chen X, Wu S, Zhou J. 2013. Influence of porosity on compressive and tensile strength of cement mortar. *Constr Build Mater* 40: 869-874. https://doi.org/10.1016/j.conbuildmat.2012.11.072
10. Chinchillas-Chinchillas MJ, Rosas-Casarez CA, Arredondo-Rea SP, Gómez-Soberón JM, Corral-Higuera R. 2019. SEM image analysis in permeable recycled concretes with silica fume. A quantitative comparison of porosity and the ITZ. *Materials* 12(13): 2201. https://doi.org/10.3390/ma12132201
11. Ziel R, Haus A, Tulke A. 2008. Quantification of the pore size distribution (porosity profiles) in microfiltration membranes by SEM, TEM and computer image analysis. *J Membr Sci* 323(2): 241-246. https://doi.org/10.1016/j.memsci.2008.05.057
12. El Boukili G, Lechheb M, Ouakarrouch M, Dekayir A, Kifani-Sahban F, et al. 2021. Mineralogical, physico-chemical and technological characterization of clay from Bensmim (Morocco): suitability for building application. *Constr Build Mater* 280: 122300. https://doi.org/10.1016/j.conbuildmat.2021.122300
13. El Boukili G, Ouakarrouch M, Lechheb M, Kifani-Sahban F, Khaldoune A. 2021. Recycling of olive pomace bottom ash (by-product of the clay brick industry) for manufacturing sustainable fired clay bricks. *Silicon* 14: 4849-4863. https://doi.org/10.1007/s12633-021-01279-x
14. Limami H, Manssouri I, Cherkaoui K, Khaldoun A. 2020. Study of the suitability of unfired clay bricks with polymeric HDPE & PET wastes additives as a construction material. *J Build Eng* 27: 100956. https://doi.org/10.1016/j.jobe.2019.100956
15. Limami H, Manssouri I, Noureddine O, Lehleh Y, Cherkaoui K, et al. 2022. Thermophysical and mechanical assessment of unfired clay bricks with dry grass fibrous filler. *Int J Thermophys* 43(8): 114. https://doi.org/10.1007/s10765-022-03043-8
16. Limami H, Manssouri I, Noureddine O, Erba S, Sahbi H, et al. 2023. Thermal study of clay bricks reinforced by dry-grass fibers. *J Energy Eng* 149(1): 04022052. https://doi.org/10.1061/JLEED9.EYENG-4613
17. Noureddine O, Manssouri I, Cherkaoui K, Sahbi H, Limami H, et al. 2022. Utilization of recycled almond wastes as additives in unfired clay bricks. *Innov Infrastruct Solut* 7(6): 335. https://doi.org/10.1007/s41062-022-00936-3
18. Prgomet I, Gonçalves B, Domínguez-Perles R, Pascual-Seva N, Barros AI. 2017. Valorization challenges to almond residues: phytochemical composition and functional application. *Molecules* 22(10): 1774. https://doi.org/10.3390/molecules22101774
19. Mkaouar S, Maherzi W, Pizette P, Zaitan H, Benzina M. 2019. A comparative study of natural Tunisian clay types in the formulation of compacted earth blocks. *J African Earth Sci* 160: 103620. https://doi.org/10.1016/j.jafrearsci.2019.103620
20. Spearing SM, Evans AG. 1992. The role of fiber bridging in the delamination resistance of fiber-reinforced composites. *Acta Metall Mater* 40(9): 2191-2199. https://doi.org/10.1016/0956-7151(92)90137-4
21. Ural N. 2021. The significance of scanning electron microscopy (SEM) analysis on the microstructure of improved clay: an overview. *Open Geosci* 13(1): 197-218. https://doi.org/10.1515/geo-2020-0145
22. Salih MM, Osofero AI, Imbabi MS. 2020. Critical review of recent development in fiber reinforced adobe bricks for sustainable construction. *Front Struct Civil Eng* 14: 839-854. https://doi.org/10.1007/s11709-020-0630-7
23. Jannat N, Al-Mufti RL, Hussien A, Abdullah B, Cotgrave A. 2021. Utilisation of nut shell wastes in brick, mortar and concrete: a review. *Constr Build Mater* 293: 123546. https://doi.org/10.1016/j.conbuildmat.2021.123546
24. Al-Fakih A, Mohammed BS, Liew MS, Nikbakht E. 2019. Incorporation of waste materials in the manufacture of masonry bricks: an update review. *J Build Eng* 21: 37-54. https://doi.org/10.1016/j.jobe.2018.09.023
25. Velasco B, Gordo E, Hu L, Radovic M, Tsipas SA. 2018. Influence of porosity on elastic properties of Ti_2AlC and Ti_3SiC_2 MAX phase foams. *J Alloys Compd* 764: 24-35. https://doi.org/10.1016/j.jallcom.2018.06.027